



**HAL**  
open science

## Hybrid materials from tri-aryl amine organogelators and poly[vinyl chloride] networks

Bethelihim Kiflemariam, Dominique Collin, Odile Gavat, Alain Carvalho, Emilie Moulin, Nicolas Giuseppone, Jean-Michel Guenet

### ► To cite this version:

Bethelihim Kiflemariam, Dominique Collin, Odile Gavat, Alain Carvalho, Emilie Moulin, et al.. Hybrid materials from tri-aryl amine organogelators and poly[vinyl chloride] networks. *Polymer*, 2020, 207, pp.122814. 10.1016/j.polymer.2020.122814 . hal-03014821

**HAL Id: hal-03014821**

**<https://hal.science/hal-03014821v1>**

Submitted on 19 Nov 2020

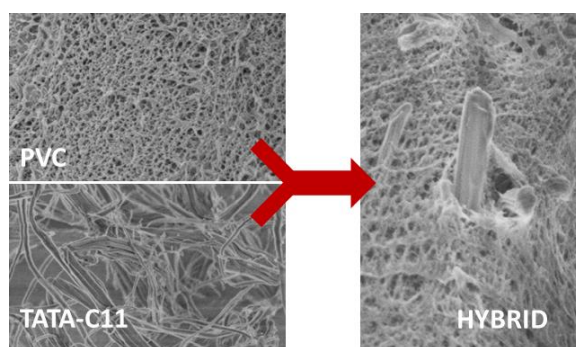
**HAL** is a multi-disciplinary open access archive for the deposit and dissemination of scientific research documents, whether they are published or not. The documents may come from teaching and research institutions in France or abroad, or from public or private research centers.

L'archive ouverte pluridisciplinaire **HAL**, est destinée au dépôt et à la diffusion de documents scientifiques de niveau recherche, publiés ou non, émanant des établissements d'enseignement et de recherche français ou étrangers, des laboratoires publics ou privés.

# HYBRID MATERIALS FROM TRI-ARYL AMINE ORGANOGELATORS AND POLY[VINYL CHLORIDE] NETWORKS.

KIFLEMARIAM, Bethelihim; COLLIN, Dominique; GAVAT, Odile; CARVALHO, Alain;  
MOULIN, Emilie; GIUSEPPONE, Nicolas; GUENET, Jean-Michel.\*

Institut Charles Sadron  
CNRS-Université de Strasbourg  
23 rue du Loess, BP84047  
67034 STRASBOURG, Cedex2, FRANCE



**Corresponding author:** Jean-Michel GUENET [jean-michel.guenet@ics-cnrs.unistra.fr](mailto:jean-michel.guenet@ics-cnrs.unistra.fr)

**Keywords :** hybrid materials, PVC, thermoreversible gels, organogels, rheology

**Abstract:** Hybrid thermoreversible gels have been prepared from polyvinyl chloride (PVC) and tri-aryl tri-amines organogelators (TATA-C11) in bromobenzene. A thermodynamic investigation by DSC has shown that the TATA-C11 formation and melting temperatures are not altered by the presence of PVC chains, nor are the formation and melting enthalpies. Scanning electron microscopy observations have revealed as each network are clearly distinguished, so that the hybrid gel is simply a combination at the micron level of both original gels. X-ray diffraction experiments have shown that the TATA-C11 structure in bromobenzene differs from its solid state, and is rather reminiscent of a hexatic phase, possibly due to the occurrence of a molecular compound. The structure of the TATA-C11 moiety does not change in the hybrid gel. Finally, the rheological properties have been studied. It is observed that the modulus of the hybrid gel greatly exceeds the Voigt's upper limit (larger than a simple additivity of the moduli). This effect is examined in the light of a possible de-solvation of the amorphous part of the PVC fibrils (de-plasticization).

## INTRODUCTION

It has been shown in a series of papers that hybrid thermoreversible networks from covalent polymers and low molecular weight molecules (or organogelators), can be straightforwardly prepared from ternary solutions after quenching at an appropriate temperature<sup>1-4</sup>. This approach represents a new path for imparting a functional property to polymers materials thanks to the presence of the organogel moiety. Only physical processes are at play such as liquid-liquid phase separation, liquid-solid transitions, liquid-solvated compound transition. The resulting gels consist of an intermingled array of fibrils of both components.

Polyvinyl chloride, PVC, is the third-most widely produced synthetic polymer. Preparing materials from this polymer with improved and/or new properties may have therefore potential applications in textile fibers<sup>5</sup> and/or porous materials<sup>6</sup>. An interesting, and quite unique property of this polymer lies in its propensity of producing thermoreversible gels of fibrillar morphology in a large variety of solvents<sup>7-13</sup>. In a recent paper, Zoukal et al. have reported the possibility of making PVC/oligophenylene vinylene (PVC/OPV) gels that bear an opto-electronic functionality, while also displaying enhanced mechanical properties<sup>4</sup>. A strong reinforcement of the gel modulus is observed with only low amounts of OPV. The modulus of the hybrid gel reaches the upper Voigt limit, namely the sum of the modulus of each constituent.

The hybrid gel formation in these PVC/OPV systems takes place in two steps: PVC gel formation occurs first, and then OPV organogel sets in. This means that the OPV gel fibrils have to grow within a confined space as the PVC gel mesh size is about 300 nm. This value is significantly lower than the OPV fibrils cross-section seen in the binary system. Although the OPV moiety has formed organized structures as ascertained by the DSC experiments, these cannot be distinguished by SEM investigations.

A question of interest is to find out what happens if the organogel forms first well before PVC gelation sets in. Thanks to the wealth of available organogelators, it becomes possible to study

systems complying with such a situation<sup>14-17</sup>. The results presented in this paper have focused on tri-arylamine tri-amine molecules (TATA-C11, see figure 1) whose gels form significantly above that of PVC in bromobenzene. In addition, the organogels from TATA-C11 possess high conducting properties, which opens up possibilities for imparting conductivity to a PVC-made material<sup>18-22</sup>.

In this paper, the investigations are restricted to the formation of the ternary gels through the mapping of the T-C phase diagrams, the determination of their molecular structure and morphology, and the investigation of their rheological properties.

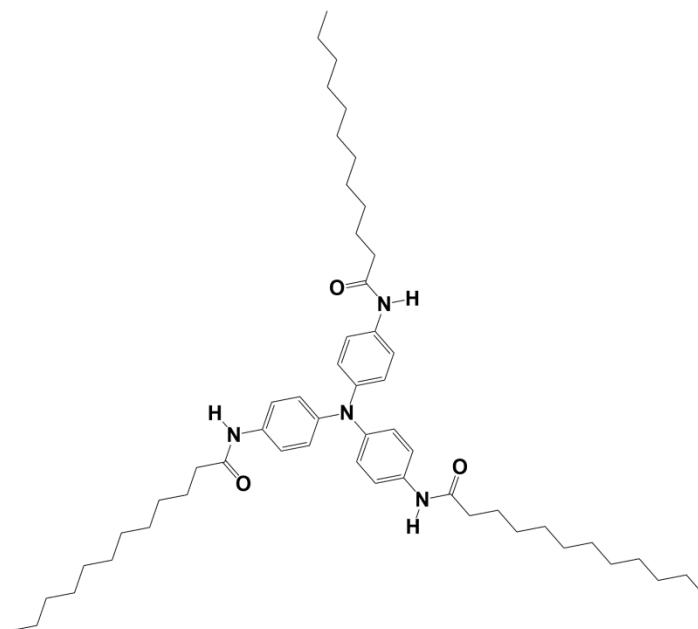


**Figure 1:** Chemical structure of TATA-C11

## EXPERIMENTAL SECTION

### *Materials*

The PVC used in the present study was purchased from Sigma-Aldrich and was used as-received. The weight average molecular weight as determined by SEC in THF at 25°C (universal calibration) is  $M_w = 7.9 \times 10^4$  g/mol and the polydispersity index  $M_w/M_n = 1.87$ . The fractions of tetrads obtained by <sup>13</sup>C-NMR are: sss=41% ssi, iss, sis,... = 39% and iii= 19%.

The fibrillar organogels were obtained from solutions of *tri-aryl tri-amines* designated as TATA-C11 in what follows (see figure 1). The synthesis and properties of these molecules are extensively described in references 18-22.

Bromobenzene, from SigmaAldrich (purity grade 99.5%), was used throughout this study without further purification.

The preparation of the binary gels (PVC/bromobenzene, TATA-C11/bromobenzene) and of the hybrid networks (PVC/TATA-C11/bromobenzene) is quite straightforward: mixtures are prepared at the desired concentration, and then heated up to 120-140°C until clear, homogeneous solutions are obtained. These solutions are quenched at low temperature (0°C down to -20°C) for producing the gels.

Two PVC concentrations have been studied:  $4.8 \times 10^{-2}$  g/cm<sup>3</sup> (or  $3.2 \times 10^{-2}$  in g/g), designated as PVC5%, and  $9.32 \times 10^{-2}$  g/cm<sup>3</sup> (or  $6.25 \times 10^{-2}$  in g/g) designated as PVC10%, while the TATA concentration was varied from  $0.5 \times 10^{-2}$  g/cm<sup>3</sup> (or 0.004 g/g) to  $1.04 \times 10^{-2}$  g/cm<sup>3</sup> (or 0.065 g/g).

### *Differential Scanning Calorimetry*

Gel formation and melting temperatures of the TATA-C11 moiety were determined by means of a DSC 8500 from Perkin Elmer. Three heating and cooling rates were used, namely 5°C/min, 10°C/min and 15°C/min within a temperature range from -20°C to 140°C. The associated enthalpies were determined from the average values obtained at the different heating rates.

Although gel formation arises from the crystallization of the longest syndiotactic sequences, the

thermal behaviour of PVC gels cannot be observed by DSC as has been already reported in several papers<sup>9,23</sup>. As a result, PVC gel formation was determined by rheological experiments by taking the gel point at the temperature where  $G' = G''$  for cooling rates close to that used for mapping out the T-C phase diagram (namely  $\sim -5^\circ\text{C}/\text{min}$ ).

Samples containing TATA-C11 were prepared as described above. About 30-40 mg of gel were introduced into stainless steel pans that were hermetically sealed by means of an o-ring. Before proceeding with the entire heating-cooling cycle a first run was systematically performed with the aim of erasing the sample history, as well as to suppress parasitic mechanical effects at the gel melting<sup>13</sup>. The weight of the sample was systematically checked after completion of the different cycles in order to evaluate any solvent loss.

### ***Scanning Electron Microscopy***

Samples were investigated by means of a FEG-cryoSEM from Hitachi (SU8010) at 1keV and at  $T = -150^\circ\text{C}$ . The images were taken with the SE-in lens detector. A piece of a gel from PVC/Bromobenzene or PVC/TATA-C11/bromobenzene was placed onto a cryo-holder and quickly plunged into a nitrogen slush in the cryo preparation chamber of a Quorum PT 3010 machine. After transferring the sample under vacuum into the chamber attached to the microscope the frozen sample was coated with a thin Pt layer (by sputter deposition) and was fractured with a razor blade. Subsequent etching was carried out at  $T = -100^\circ\text{C}$  so as to reveal the details of the morphology.

### **X-ray diffraction**

WAXS were performed by means of a Nanostar diffractometer from Bruker-Anton Paar that operates with a pinhole collimator and a wire-proportional gas detector. A monochromatic beam ( $\lambda = 0.154 \text{ nm}$  from  $\text{Cu K}\alpha_1$ , with a divergence  $= 0.03^\circ$ ) was obtained by shining the primary beam onto a confocal mirror with advanced W/Si multilayer coating (XENOCS, SA). The size of the incident beam on the sample was about  $300 \mu\text{m}$ . The sample to detector distance was set in such a way as to access scattering vectors ( $q = 4\pi\sin(\theta/2)/\lambda$  where  $\theta$  is the diffraction angle) ranging from

$q = 0.5$  to  $30 \text{ nm}^{-1}$ . Data reduction was carried out following the standard procedure for isotropic scattering. An iron source was used for correcting cell efficiency and determining the solid angle. Calibration of the scattering vector scale was achieved with a silver Behenate sample. Cells of 1 mm thickness made up with calibrated Mica windows were used as sample holders.

### ***Rheology***

The real and imaginary parts of the complex shear modulus were measured with a stress-controlled rheometer (Haake, Mars III) operating in the oscillatory mode. The complex modulus as a function of frequency, on the one hand, and the gelation temperature at constant frequency, on the other hand, were determined by means of a double Couette cell (DG41, Haake) with a gap of  $\sim 400 \mu\text{m}$ . Approximately  $7 \text{ cm}^3$  of the hot solution were necessary for the experiments. The temperature in the Couette cell was monitored by means of an external bath (Haake F3). For all the shear measurements the applied stresses were lower than  $\sigma = 5 \times 10^{-2} \text{ Pa}$  so as to remain within the linear regime.



## RESULTS AND DISCUSSION

### 1) Thermodynamic, structure and morphology of the binary gels.

The formation and melting temperatures of the organogels from the TATA-C11 molecules have been first studied by DSC as a function of both concentration  $X_{\text{TATA}}$  (in g/g) and heating-cooling rates. The corresponding temperature-concentration phase diagram has been mapped out for heating-cooling rates of 5°C/min (figure 2a). A fit is performed with a polynomial of degree 3, which has no theoretical basis but only serves as a guide for the eyes. Typically, TATA-C11 gel formation occurs above 80°C in the investigated concentration range. The values of the associated enthalpies are also reported in figure 2left by means of a Tamman's plot. As can be seen, formation and melting enthalpies are virtually identical, which implies that no significant kinetic effects are present, namely gel formation is essentially instantaneous. The results are fitted with a straight line going through the origin as required from the Gibbs phase rules. Interestingly, the extrapolation to  $X_{\text{TATA}} = 1$  yields  $\Delta H = 28$  J/g which is at variance with the value measured for the pure TATA-C11 ( $\Delta H = 53$  J/g.). In view of the shape of the phase diagram, the concentration of TATA-C11 in the liquid phase is negligible, so that this enthalpy value does not result in the existence of non-gelled molecules (see sup. info. figure S1). This outcome rather suggests that the molecular structure of the gel state differs from that of the solid state, a statement confirmed by the X-ray experiments.

The diffraction pattern of the TATA-C11 solid state displays several peaks, which corresponds to that of a crystalline material. Conversely, the diffraction pattern of the gel state exhibits only one narrow peak at  $q = 1.92 \text{ nm}^{-1}$ , and a broad maximum at  $q = 16.6 \text{ nm}^{-1}$ , the latter arising from the liquid scattering of the solvent. The distance associated with the narrow peak calculated with Bragg's law ( $d = 3.28 \text{ nm}$ ) is larger than that corresponding to the first peak observed in the solid state ( $d = 2.54 \text{ nm}$ ). The diffraction pattern of the gel state is reminiscent of that observed for hexatic mesophases in liquid crystals. This possibly means that there is a high short-range order that is rapidly lost over larger distances. Further, the large distance associated with the narrow peak may

suggest the occurrence of TATA-C11/bromobenzene co-crystals in the gel state<sup>24</sup>. This assumption

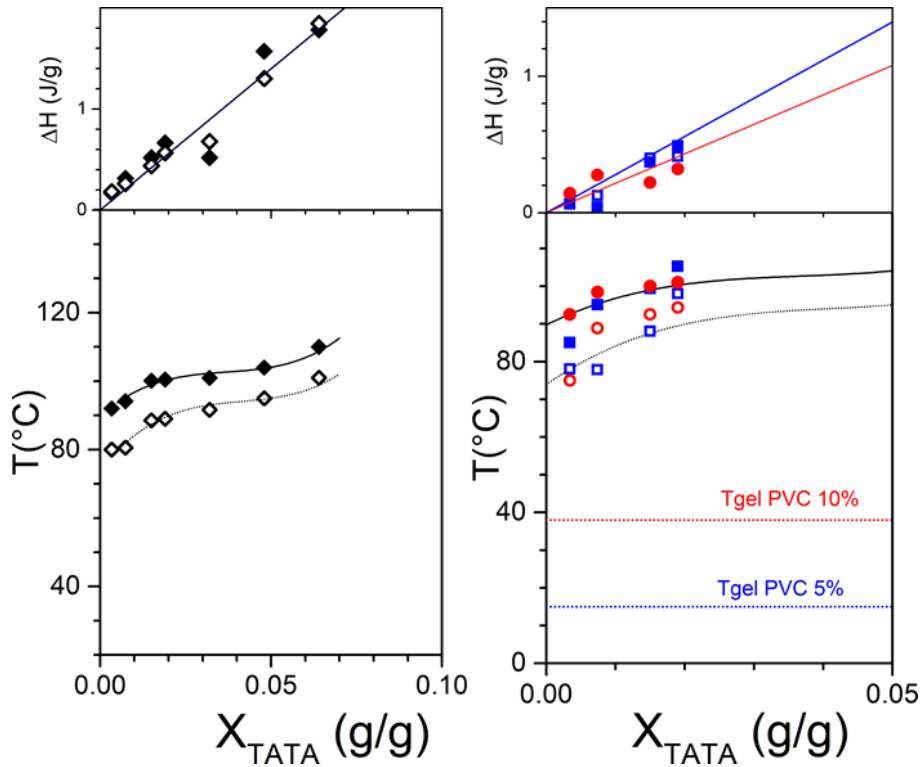


**Figure 2:** *left:* Temperature-concentration phase diagram for TATA-C11/bromobenzene. ( $\blacklozenge$ )= gel melting temperature; ( $\diamond$ )= gel formation temperature. The full line and dotted lines stand for a fit with a polynomial of degree 3, which only serves as a guide for the eyes. Upper plot: Tamman's diagram of the corresponding enthalpies. **Right:** Temperature-concentration phase diagram for PVC/TATA-C11/bromobenzene; ( $\blacksquare$ )= TATA-C11 melting with PVC5%, ( $\square$ )=TATA-C11 formation with PVC5%, ( $\bullet$ ) TATA-C11 melting with PVC10%, ( $\circ$ ) TATA-C11 formation with PVC10%. For the sake of clarity, the experimental points for TATA-C11/bromobenzene are not shown but only the dotted and full lines obtained from the polynomial fits in the left diagram. The gelation temperatures of PVC5% and PVC10% for a fast cooling rate are also shown. Upper plot: Tamman's diagram; the blue straight line is a fit for the PVC5%TATA-C11 gels, while the red line is a fit for the PVC10%/TATA-C11 gels.

is consistent with the lower melting-formation enthalpies measured by DSC.

As aforementioned, PVC gels cannot be studied by DSC as no formation exotherm nor melting endotherm are observed<sup>13</sup>. This arises chiefly from two effects: i) the low amount of long enough syndiotactic sequences responsible for the growth of the crystalline junctions, and correspondingly

the low degree of crystallinity (max. 5%); and ii) the spread of the thermal events over a large temperature domain. The gelation temperatures have been therefore determined by oscillatory rheological experiments when  $G' = G''$  (see supp. info S2) **by cooling rapidly the Couette cell so as to reach a rate close enough to that used for mapping out the phase diagram. Under these conditions, the cooling rate does not remain constant throughout the temperature scan. It varies from 3°C/min at high temperature down to 0.7°C/min at low temperature (see supp. info. figure S3).**

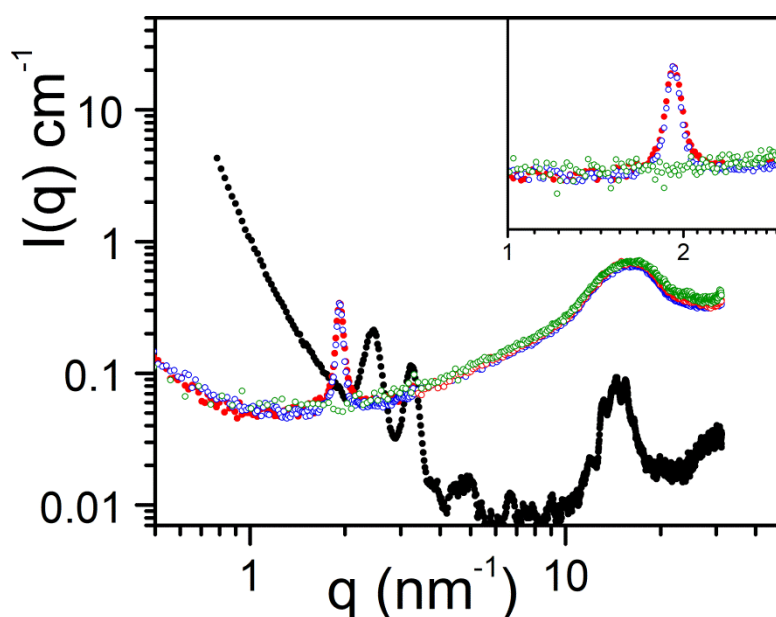


**Figure 3:** X-ray diffraction patterns for: TATA-C11 in the solid crystalline state (●); TATA-C11/bromobenzene gel at 2% (●); PVC10%/TATA-C11/bromobenzene 10%/2% (●); PVC10% (●). Inset: blow-up for the diffraction patterns of the three different gels in the peak domain.

**The results are:**  $T_{\text{gel}} = 15 \pm 3^\circ\text{C}$  for PVC5% and  $T_{\text{gel}} = 37 \pm 2^\circ\text{C}$  for PVC10%. Thus, PVC gels always form at lower temperature than the TATA-C11 organogels at fast cooling rates. Yet, the PVC gelation temperature depends drastically upon the cooling rate. Cooling at 0.25°C/min increases the gelation temperature by about 50°C for PVC5% and about 33°C for PVC10%. PVC gel formation remains, however, under the TATA-C11 gelation point.

Unlike the TATA-C11 gels, the PVC10% diffraction pattern is featureless except for the maximum at  $q = 16.6 \text{ nm}^{-1}$  due to the solvent scattering (figure 3). This arises from the low intrinsic

crystallinity of the PVC material (estimated to be about 5%<sup>11</sup>) so that the observation of diffraction peaks is not expected for a 10% gel.

The typical morphology of the PVC gels in bromobenzene is shown in figure 4a. It consists of a network of fibrils possessing cross-section in the range 30-100 nm with an average mesh size of about 300 nm<sup>21</sup>. The morphology of the TATA-C11 gels observed by SEM is shown in figure 4b.

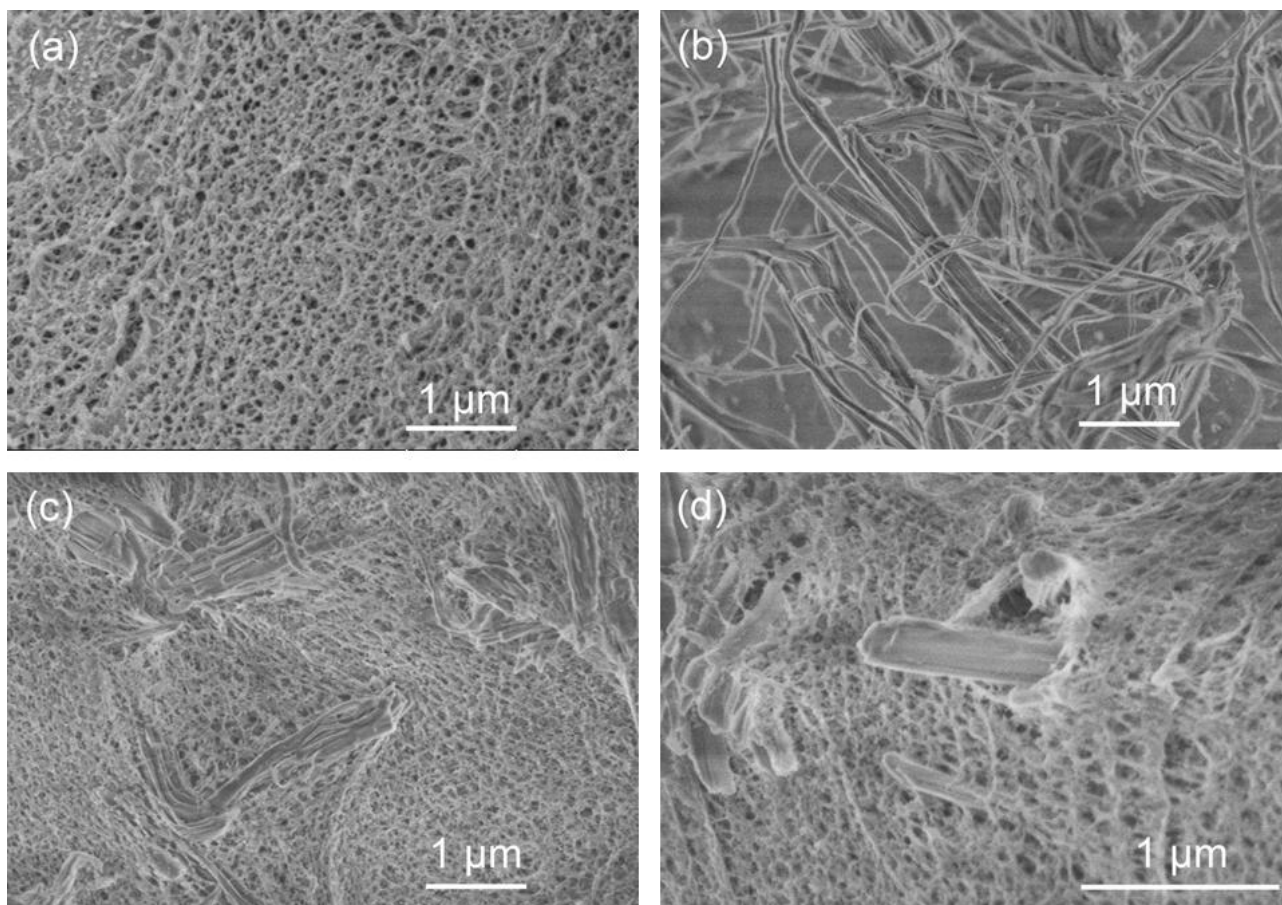


**Figure 4:** CryoSEM micrographs for gels in bromobenzene: (a) PVC5%; (b) TATA-C11 2%; (c) and (d) PVC5%/TATA-C11/bromobenzene.

The micrograph displays a rather disordered network made up with fibrils and ribbon-like structures of cross-sections ranging from 40 to 500 nm. Unlike PVC gels, estimating a mesh size is meaningless for two reasons: i) one cannot clearly observe junctions, such as fibrils merging together, but rather a jumble of non-connected fibrils; ii) the space between fibrils varies from a few nanometers up to a few micrometers.

## 2) Thermodynamic, structure and morphology of the hybrid gels.

Investigations by DSC on the ternary systems were restricted to the formation and melting of the TATA-C11 moiety since, as explained above, the PVC thermograms are featureless. Two PVC concentrations were used (5% and 10%), while the TATA-C11 concentrations were ranging from  $0.5 \times 10^{-2} \text{ g/cm}^3$  (or 0.004 g/g) to  $1.04 \times 10^{-2} \text{ g/cm}^3$  (or 0.065 g/g). As can be seen in figure 2left, there is virtually no effect on the thermodynamic properties of the TATA-C11 component in the presence of PVC. Whether the PVC gel forms first, as with OPV organogelators, or forms last, as discussed herein, does not change the thermodynamic behavior of the organogel moiety.

The absence of modification of the TATA-C11 gelation properties is further backed up by the occurrence of the same narrow peak in the diffraction pattern, at the same position with nearly the same magnitude (figure 3).

The morphology as revealed by SEM observations consists of TATA-C11 fibrils embedded in the PVC gel (figure 4). The shape and size of the TATA-C11 fibrils are similar to those in the binary system, which is consistent with the conservation of their thermodynamic properties in the hybrid network. Similarly, the mesh size of the PVC network is unaltered by the presence of the TATA-C11 fibrils (figure5).

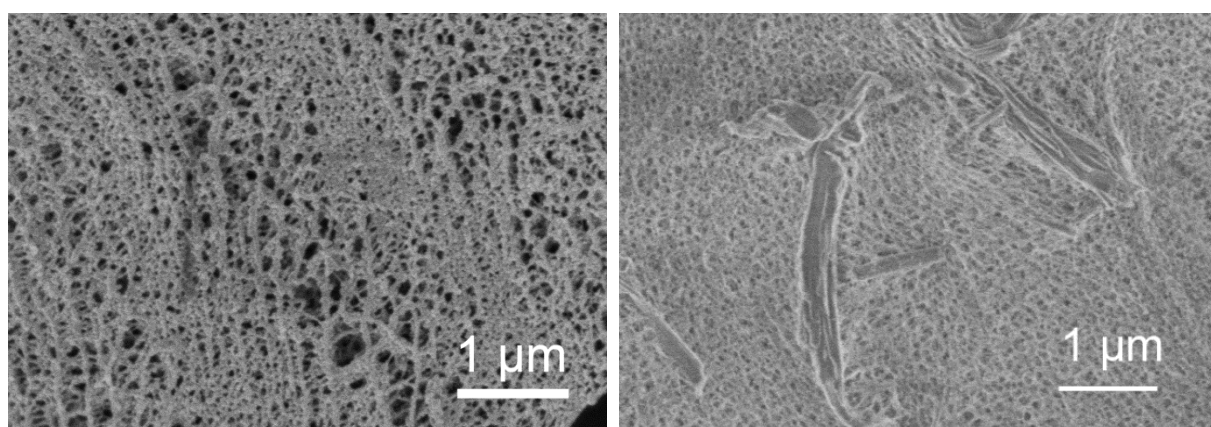


**Figure 5:** *left* : OPV/PVC/Bromobenzene gels (from ref. 4); *right* TATA-C11/PVC gels. In the latter case the different networks can easily be identified.

These outcomes are at variance with the previously studied system (OPV/PVC)<sup>4</sup> wherein the OPV fibrils could not be clearly identified, although their thermodynamic properties were unchanged. This difference probably arises from the spatial environment where the fibrils of the second gel grow. In the ternary system PVC/OPV, the OPV fibrils must form within “tunnels” of size smaller than their cross-sections, whereas in the system PVC/TATA-C11 the PVC gel is allowed to form in a much more open network. As a result, both networks are easily distinguishable in this case.

### 3) Rheology.

We have observed in the hybrid gels prepared from PVC/OPV/bromobenzene mixtures that the elastic modulus is simply the sum of the modulus of each moiety as determined from their binary gels. Thus, the system obeys the so-called Voigt's upper limit, which, in principle, cannot be exceeded. Herein, we have studied both the variation of the complex modulus during gel formation, and the elastic modulus measured at a constant temperature. As expected,  $G'$  is a constant in the explored frequency range, and at least one order of magnitude larger than  $G''$  (figure S4 supp. Info.) The PVC gel formation is shown in figure 6 (upper left). As can be seen the gelation process starts at  $T_o \approx 52 \pm 3^\circ\text{C}$ , which corresponds to the formation of finite aggregates, and gelation, namely appearance of infinite aggregates, occurs at  $T_{gel} \approx 13^\circ\text{C}$  where  $G' = G''$ .

As expected from the DSC results, the organogel TATA-C11/Bromobenzene forms at higher temperature  $T_{gel} \approx 77^\circ\text{C}$  where  $G' = G''$  (figure 6 upper right). Unlike the PVC gels  $T_{gel} \approx T_o$  which means that infinite aggregates form almost immediately. Yet, at  $T_{end} \approx 52^\circ\text{C}$  the curves of  $G'$  and  $G''$  exhibit a cusp, which is possibly related to the end of the DSC exotherm (see sup. info.figure S5).

The formation of the complex modulus of the hybrid gel is a simple combination of the sequences observed in the binary systems. The gel point of the entire system,  $T_{gel} \approx 72^\circ\text{C}$ , corresponds to the gelation temperature of the TATA-C11/bromobenzene gel, the cusp occurs at the same temperature  $T_{end} \approx 52^\circ\text{C}$ . Then, the elastic modulus  $G'$  and the loss modulus  $G''$  both increase at the same rate. This means that more elastic material is formed, but also that there remains a viscous material

which is mainly the PVC chains and aggregates. Finally, the gelation of the PVC chains takes place at about  $T_{\text{gelPVC}} \approx 18^\circ\text{C}$  together with a significant increase of the gel elastic modulus while  $G''$  finally becomes constant. The behaviour for a hybrid gel containing more TATA molecules (PVC/TATA 5%/2%) is basically the same (see figure 6 and sup. info S6 for TATA/2%).

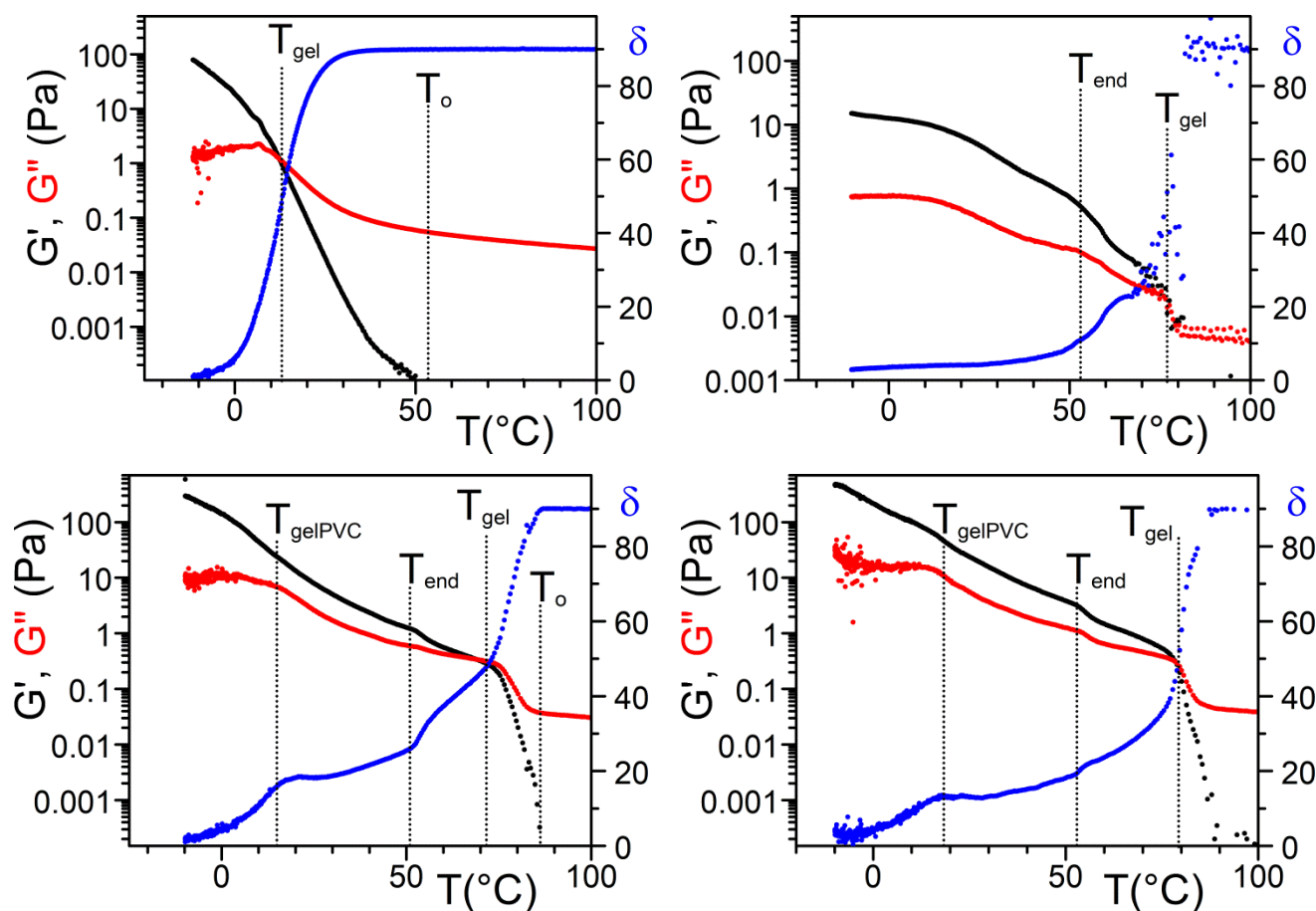


**Figure 6:** Variation of the elastic modulus,  $G'$  (●), the loss modulus,  $G''$  (●) and the phase shift  $\delta$  (●) determined at fast cooling (see figure SXX). **Upper left:** PVC5%/bromobenzene system, **upper right:** TATA-C11/bromobenzene 1% systems; **lower left:** the PVC/TATA-C11/bromobenzene systems (5%/1%); **lower right:** PVC/TATA-C11/bromobenzene systems (5%/2%) Remarkable temperatures are indicated (see text for details).

The rheological behaviour confirms therefore the findings by DSC, X-ray diffraction and SEM, namely the hybrid gel is a combination of the binary systems, where the organogel and the PVC network keep their structures and properties.

Another interesting outcome from these experiments is the unexpected high values of the elastic modulus that are listed in table 1.

	PVC5% ( $4.8 \times 10^{-2}$ )	1% TATA-C11 (0.01)	PVC/TATA-C11 5%/1% ( $4.8 \times 10^{-2}/0.01$ )	2% TATA-C11 (0.02)	PVC/TATA-C11 5%/2% ( $4.8 \times 10^{-2}/0.02$ )
0°C	19±2	12±4	139±10	108	200
-10°C	67.5±3	15±2	295±20	190	500

**Table 1:**  $G'$  in Pa for the TATA-C11 organogel, the PVC gel and the hybrid PVC/TATA-C11/bromobenzene gel (5%/1%, and 5%/2%) at 0°C and -10°C. (Concentrations in g/cm<sup>3</sup> are given in brackets).

For the 5%/1% system, the hybrid gel possesses an elastic modulus that greatly exceeds Voigt's upper limit, unlike what has been observed with the PVC/OPV gels<sup>4</sup>. This effect is still there for the 5%/2% system yet is less pronounced, chiefly because the TATA2% gel modulus is about 10 times larger than that of the TATA1% gel. Incidentally, this suggests that the power law variation of the TATA gel modulus with concentration requires an exponent of about 3. Usually, for fibrillary gels an exponent close to 2 is measured<sup>16</sup>. A possible explanation for this discrepancy may arise from the existence of a large fraction of pendent fibrils at low concentration, namely fibrils not participating in the gel elasticity, which entails an apparent exponent larger than 2.

The previous section has led one to the conclusion that the hybrid gel is essentially a combination of the binary systems. The thermal properties of the TATA-C11 are unchanged, nor is their structure, and the morphology of the PVC gel is basically the same. In principle, exceeding Voigt's upper limit should not be not possible unless the rigidity of one of the component is altered.

A similar behaviour has already been observed with graphene and/or graphene oxide dispersed into a PMMA matrix. At ultralow loadings (<0.50 vol %) one observes a strong reinforcement of the mechanical properties of the polymer nanocomposites<sup>26-28</sup>. The effect was attributed by some authors to hydrogen-bonding interaction or to an interlocking due to the wrinkled morphology of



graphene. Li and McKenna<sup>29</sup> have demonstrated that ultralow loadings of graphene oxide raises the glass transition temperature  $T_g$  of the composite, possibly by a de-plasticization process, which leads to an increase of the elastic modulus.

We suspect that a similar process may be at play in our systems. One must keep in mind that the elastic properties of a network depend on two parameters: the number of junction per unit volume, and the intrinsic elastic modulus of the fibrils<sup>30</sup>. Studies on the molecular structure of PVC gels<sup>31,32</sup> have shown that their fibrils are chiefly made up with three entities: i) highly syndiotactic sequences responsible for the crystalline junctions that appear at the onset of gelation, ii) synditactic sequences with a few stereoregular defects that form PVC/solvent complexes, and are responsible for the gel ageing<sup>33</sup>, and iii) domains of more or less solvated heterotactic sequences, or in other words plasticized amorphous domains (see figure 6). If the presence of TATA-C11 molecules would trigger de-solvation of the amorphous domains of the PVC fibrils by changing solvent quality, then their intrinsic elastic modulus might drastically increase, and so would the elastic modulus of the hybrid gel (figure 6). This effect is therefore similar to an increase of  $T_g$  as highlighted by Li and McKenna<sup>29</sup>.

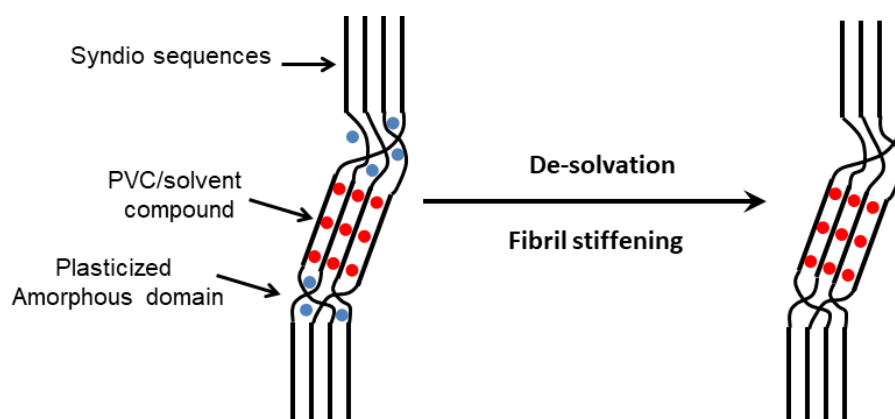


**Figure 7:** Schematic representation of the different types or organization within a PVC fibril. The de-solvation process is supposed to modify the content of solvent molecules in the amorphous domains of the fibrils, hence an increase of their rigidity.

We cannot, however, totally disregard the possible creation of additional junctions, or the

involvement of more PVC chains in the elastic material (decrease of the fraction of pendent chains and/or of free chains, for instance). This would still be related to the alteration of solvent quality by the TATA-C11 molecules.

The experiments reported by Najeh et al.<sup>33</sup> may give some hint as to the magnitude of the solvent quality effect required for observing an increase of modulus. These authors have determined that the gel modulus vs solvent quality varies as  $E \sim G^{2.72}$  where  $G$  is the swelling ratio ( $G = V/V_0$ ). On this basis, a de-swelling ratio of about 1.5 accounts for a threefold increase of the modulus, since PVC gel moduli vary<sup>11</sup> as  $G \sim C^3$  (this corresponds to a 1.14 change in dimension). Clearly, a slight change in solvent quality may drastically modify the elastic modulus.

We further note that the elastic modulus of the 5%/2% system turns out to be approximately the sum of the 5%/1% system and the TATA2% moduli. This may suggest that the de-plasticization effect has already reached a maximum for TATA1%, so that Voigt's limit is retrieved for higher TATA concentrations as was observed with PVC/OPV systems<sup>4</sup>.

### **Concluding remarks**

In this paper, we have shown that the formation of a hybrid gel involving a covalent polymer and an organogelator is easily achievable by mixing the components at elevated temperature followed by an appropriate quench. Here, the organogel forms first so that the PVC gel fibrils are allowed to grow in a rather open space as opposed to a previous studied system prepared from PVC/oligo phenylene-vinylene molecules. This results in a clear, unmistakable identification of each network by scanning electron microscopy. The thermodynamic properties and the molecular structure of the TATA-C11 moiety are not altered in the hybrid system. The resulting hybrid gel is therefore a simple combination of each network. Conversely, the rheological properties do not comply to this scheme. The elastic modulus exceeds greatly the Voigt's upper limit, namely it is far larger than the addition of the modulus of each constituent. We have attempted to explain this effect by

contemplating a hypothetical change of rigidity of the PVC fibrils through a de-plasticization process in the light of recent findings by Li and McKenna<sup>29</sup>. This effect could arise from a modification of solvent quality towards PVC triggered by the presence of the TATA-C11 molecules.

**Corresponding Author:** jean-michel.guenet@ics-cnrs.unistra.fr; ORCID 0000-0002-3829-8303

**Note:** The authors declare no competing financial interest

**CRedit author statement:** investigation: B.K., D.C, A.C. O.D. validation: E.M., N.G. conceptualization and supervision J.M.G.

**Acknowledgments:** The authors are indebted to C. Saettel for the DSC investigations, to G. Fleith for the X-ray diffraction experiments, and to M-C. Samy-Arlaye for her support in the synthesis of the TATA molecules. Stimulating discussions for SEM investigations with M. Schmutz are also highly appreciated. The authors are greatly indebted to G. B. McKenna for pointing us to cases where the elastic modulus can exceed Voigt's upper limit.

**REFERENCES**

- 1) Dasgupta, D.; Srinivasan, S.; Rochas, C.; Ajayaghosh, A.; Guenet, J.M. Hybrid thermoreversible gels from covalent polymers and organogels *Langmuir* **2009**, *25*, 8593;
- 2) Guenet, J.M. Hybrid Physical Gels from Polymers and Self-Assembled Systems: A Novel Path for Making Functional Materials *Gels* **2018**, *4*, 35
- 3) Bairi, P.; Chakraborty, P.; Shit, A.; Mondal, S.; Roy, B.; Nandi, A.K. A Co-assembled Gel of a Pyromellitic Dianhydride Derivative and Polyaniline with Optoelectronic and Photovoltaic Properties *Langmuir* **2014**, *30*, 7547.
- 4) Zoukal, Z.; Elhasri, S.; Carvalho, A.; Schmutz, M.; Collin, D.; Vakayil, P.K.; Ajayaghosh, A.; Guenet, J.M. Hybrid materials from poly[vinyl chloride] and organogels *ACS Appl. Polym. Mater.* **2019**, *1*, 1203
- 5) see for instance <http://polymerdatabase.com/Fibers/PVC.html>
- 6) see for instance: Mei, S.; Xiao, C.; Hu, X. Preparation of porous PVC membrane via a phase inversion method from PVC/DMAc/water/additives *Appl. Polym. Sci.* **2010**, *120*, 557
- 7) See for instance Gnanou, Y.; Fontanille, M. *Organic and Physical Chemistry of Polymers*, **2008** John Wiley & Sons, , N.Y.
- 8) Stein, R.S.; Tobolsky, A.V. An investigation of the relationship between polymer structure and mechanical properties: Part II: An Experimental Study of the Stress and Birefringence Properties *Text. Res. J.* **1949** *18* 302
- 9) Alfrey, T.; Wiederhorn, N.; Stein, R.S.; Tobolsky, A.V. Some studies of plasticized polyvinylchloride *J. Colloid. Sci.* **1949**, *4*, 211.
- 10) Walter, A.T. Elastic properties of polvinyl chloride gels *J. Pol. Sci.* **1954**, *13*, 207
- 11) Juijn, J.A.; Gisolf, A.; deJong, W.A. Crystallinity in atactic poly vinyl chloride *Kolloid Z. Z. Polym.* **1973**, *251*, 456

- 12) te Nijenhuis, K.T. and Dijkstra, H. Investigation of the aging process of a polyvinyl chloride gel by the measurement of its dynamic moduli *Rheol. Acta* **1975**, *14*, 71.
- 13) Mutin, P.H.; Guenet, J.M. Physical gels from PVC: ageing and solvent effect on thermal behavior, swelling and compression modulus. *Macromolecules* **1989**, *22*, 843.
- 14) Ajayaghosh, A. and Praveen, V.K.  $\pi$ -Organogels of Self-Assembled p-Phenylenevinylenes: Soft Materials with Distinct Size, Shape, and Functions *Acc. Chem. Res.*, **2007**, *40*, 644–656.
- 15) Weiss, R.G. The past, present and future of molecular gels. What is the status of the field, and where is it going? *J. Am. Chem. Soc.* **2014**, *136*, 7519-7530
- 16) Guenet, J.M. Organogels: thermodynamics, structure, solvent role and properties, **2016**, N.Y., Springer International Publishing
- 17) *Molecular Gels, Structure and Dynamics*, Weiss, R.G. Ed., Monograph in Supramolecular Chemistry, **2018**, Royal Society of Chemistry, London
- 18) Ellis, T. K.; Galerne, M.; Armao IV, J. J.; Osypenko, A.; Martel, D.; Maaloum, M.; Fuks, G.; Gavat, O.; Moulin, E.; Giuseppone, N. Supramolecular electropolymerization *Angew. Chem. Int. Ed.* **2018**, *57*, 15749-15753.
- 19) Moulin,E.; Niess, F.; Maaloum, M.; Buhler, E.; Nyrkova, L. ; Giuseppone, N. The hierarchical self-assembly of charge nanocarriers: a highly cooperative process promoted by visible light *Angew. Chem. Int. Ed.* **2010**, *49*, 6974..
- 20) E.; Nyrkova, L. ; Moulin,E.; Armao IV, J.J.; Maaloum, M.; Heinrich, B.; Rawiso, M.; Niess, F.; Cid, J.J.; Jouault, N.; Buhler, E.; Semenov, A. Giuseppone, N. Supramolecular self-assembly and radical kinetics in conducting self-replicating nanowires. *ACS Nano* **2014**, *8*, 10111
- 21) Armao IV, J.J.; Maaloum, M.; Ellis, T.; Fuks, G.; Rawiso, M.; Moulin,E.; Giuseppone, N. Healable supramolecular polymers as organic metals *J. Am. Chem. Soc.* **2014**, *136*, 11382
- 22) Moulin,E.; Armao IV, J.J.; Giuseppone, N. Triaryl amine-based supramolecular polymers: structure, dynamics, and functions *Acc. Chem. Res.* **2019**, *52*, 975

- 23) Yang, Y.C. and Geil, P.H. Morphology and properties of PVC/solvent gels *J. Macromol. Sci.* **1983**, *B(22)*, 463
- 24) Guenet, J.M. Polymer-solvent molecular compounds, **2008**, Elsevier, London.
- 25) Ramzi, M. ; Rochas, C.; Guenet, J.M. Structure-Properties Relation for Agarose Thermoreversible Gels in Binary Solvents *Macromolecules* **1998**, *31*, 6106
- 26) Ramanathan, T.; Abdala, A. A.; Stankovich, S.; Dikin, D. A.; Herrera-Alonso, M.; Piner, R. D.; Adamson, D. H.; Schniepp, H. C.; Chen, X.; Ruoff, R. S.; Nguyen, S. T.; Aksay, I. A.; Prud'Homme, R. K.; Brinson, L. C. Functionalized graphene sheets for polymer nanocomposites. *Nat. Nanotechnol.* **2008**, *3*, 327–331.
- 27) Potts, J. R.; Lee, S. H.; Alam, T. M.; An, J.; Stoller, M. D.; Piner, R. D.; Ruoff, R. S. Thermomechanical properties of chemically modified graphene/poly(methyl methacrylate) composites made by in situ polymerization. *Carbon* **2011**, *49*, 2615–2623.
- 28) Rafiee, M. A.; Rafiee, J.; Wang, Z.; Song, H.; Yu, Z.-Z.; Koratkar, N. Enhanced Mechanical Properties of Nanocomposites at Low Graphene Content *ACS Nano* **2009**, *3*, 3884–3890.
- 29) Li, X.; McKenna, G.B. Considering Viscoelastic Micromechanics for the Reinforcement of Graphene Polymer Nanocomposites *ACS Macro Lett.* **2012**, *1*, 388
- 30) Jones, J. L.; Marques, C. M. Rigid polymer network models *J. Phys. (les Ulis)* **1990**, *51*, 1113
- 31) Abied, H.; Brûlet, A.; Guenet, J.M. Physical gels from PVC: molecular structure of pregels and gels by low angle neutron scattering *Coll. Polym. Sci.* **1990**, *268*, 403.
- 32) Lopez, D.; Dahmani, M.; Mijangos, C.; Brulet, A.; Guenet, J.M. Molecular structure by neutron scattering of thermoreversible gels from chemically-modified PVC *Macromolecules* **1994**, *27*, 7415
- 33) Najeh, M.; Munch, J.P.; Guenet, J.M. Physical gels from PVC: effect of solvent type *Macromolecules* **1992**, *25*, 7018